Polarization-sensitive characterization of the propagating plasmonic modes in silver nanowire waveguide on a glass substrate with a scanning near-field optical microscope

Priyamvada Venugopalan, Qiming Zhang, Xiangping Li, and Min Gu*

Centre for Micro-Photonics, Faculty of Engineering and Industrial Sciences, Swinburne University of Technology, Hawthorn, Victoria 3122, Australia

*mgu@swin.edu.au

Abstract: In this paper, we report on the experimental investigation of the polarization properties of the plasmonic modes along a silver nanowire waveguide on a glass substrate. Two orthogonal polarization light components at the distal end of the nanowire are observed in the far-field. The near-field mapping with a scanning near-field optical microscopic probe exhibiting an in-plane polarization sensitivity reveals the two polarization components of the propagating plasmonic modes along the nanowire.

OCIS codes: (250.5403) Plasmonics; (230.7370) Waveguides; (180.4243) Near-field microscopy.

References and links

1. E. R. Encina, E. M. Perassi, and E. A. Coronado, "Near-field enhancement of multipole plasmon resonances in Ag and Au nanowires," J. Phys. Chem. A **113**(16), 4489–4497 (2009).
2. A. Pucci, F. Neubrech, J. Aizpurua, T. Cornelius, and M. Chapelle, "Electromagnetic nanowire resonances for field-enhanced spectroscopy," in *One-Dimensional Nanostructures*, Z. Wang, ed. (Springer-New York, 2008).
3. Y. Fang, Z. Li, Y. Huang, S. Zhang, P. Nordlander, N. J. Halas, and H. Xu, "Branched silver nanowires as controllable plasmon routers," Nano Lett. **10**(5), 1950–1954 (2010).
4. S. Zhang, H. Wei, K. Bao, U. Håkanson, N. J. Halas, P. Nordlander, and H. Xu, "Chiral surface plasmon polaritons on metallic nanowires," Phys. Rev. Lett. **107**(9), 096801 (2011).
5. Q. Li, S. Wang, Y. Chen, M. Yan, L. Tong, and M. Qiu, "Experimental demonstration of plasmon propagation, coupling, and splitting in silver nanowire at 1550-nm wavelength," IEEE J. Sel. Top. Quantum Electron. **17**(4), 1107–1111 (2011).
6. S. Lal, J. H. Hafner, N. J. Halas, S. Link, and P. Nordlander, "Noble metal nanowires: from plasmon waveguides to passive and active devices," Acc. Chem. Res. **45**(11), 1887–1895 (2012).
7. X. Xiong, C.-L. Zou, X.-F. Ren, A.-P. Liu, Y.-X. Ye, F.-W. Sun, and G.-C. Guo, "Silver nanowires for photonics applications," Laser & Photo. Rev. doi: 10.1002/lpor.201200076 (2013).
8. C. L. Zou, F. W. Sun, Y. F. Xiao, C. H. Dong, X. D. Chen, J. M. Cui, Q. Gong, Z. F. Han, and G. C. Guo, "Plasmon modes of silver nanowire on a silica substrate," Appl. Phys. Lett. **97**(18), 183102 (2010).
9. S. Xie, Z. Ouyang, B. Jia, and M. Gu, "Large-size, high-uniformity, random silver nanowire networks as transparent electrodes for crystalline silicon wafer solar cells," Opt. Express **21**(S3), A355–A362 (2013).
10. Y. Wang, Y. Ma, X. Guo, and L. Tong, "Single-mode plasmonic waveguiding properties of metal nanowires with dielectric substrates," Opt. Express **20**(17), 19006–19015 (2012).
11. Q. Li and M. Qiu, "Plasmonic wave propagation in silver nanowires: guiding modes or not?" Opt. Express **21**(7), 8587–8595 (2013).
12. H. Ditlbacher, A. Hohenau, D. Wagner, U. Kreibig, M. Rogers, F. Hofer, F. R. Aussenegg, and J. R. Krenn, "Silver nanowires as surface plasmon resonators," Phys. Rev. Lett. **95**(25), 257403 (2005).
13. B. Hecht, H. Bielefeldt, L. Novotny, Y. Inouye, and D. W. Pohl, "Local excitation, scattering, and interference of surface plasmons," Phys. Rev. Lett. **77**(9), 1889–1892 (1996).
14. R. Fujimoto, A. Kaneta, K. Okamoto, M. Funato, and Y. Kawakami, "Interference of the surface plasmon polaritons with an Ag waveguide probed by dual-probe scanning near-field optical microscopy," Appl. Surf. Sci. **258**(19), 7372–7376 (2012).
15. J. K. Lim, K. Imura, T. Nagahara, S. K. Kim, and H. Okamoto, "Imaging and dispersion relations of surface plasmon modes in silver nanorods by near-field spectroscopy," Chem. Phys. Lett. **412**(1-3), 41–45 (2005).
16. Z. Li, K. Bao, Y. Fang, Y. Huang, P. Nordlander, and H. Xu, "Correlation between incident and emission polarization in nanowire surface plasmon waveguides," Nano Lett. **10**(5), 1831–1835 (2010).

#190145 - $15.00 USD Received 6 May 2013; revised 9 Jun 2013; accepted 11 Jun 2013; published 18 Jun 2013

17. J. Kottmann, O. Martin, D. Smith, and S. Schultz, "Plasmon resonances of silver nanowires with a nonregular cross section," Phys. Rev. B **64**(23), 235402 (2001).
18. A. W. Sanders, D. A. Routenberg, B. J. Wiley, Y. Xia, E. R. Dufresne, and M. A. Reed, "Observation of plasmon propagation, redirection, and fan-out in silver nanowires," Nano Lett. **6**(8), 1822–1826 (2006).
19. Z. Li, F. Hao, Y. Huang, Y. Fang, P. Nordlander, and H. Xu, "Directional light emission from propagating surface plasmons of silver nanowires," Nano Lett. **9**(12), 4383–4386 (2009).
20. P. Biagioni, D. Polli, M. Labardi, A. Pucci, G. Ruggeri, G. Cerullo, M. Finazzi, and L. Duo, "Unexpected polarization behavior at the aperture of hollow-pyramid near-field probes," Appl. Phys. Lett. **87**(22), 223112 (2005).
21. Z. Liu, J. M. Steele, W. Srituravanich, Y. Pikus, C. Sun, and X. Zhang, "Focusing surface plasmons with a plasmonic lens," Nano Lett. **5**(9), 1726–1729 (2005).
22. M. Zhang, J. Du, H. Shi, S. Yin, L. Xia, B. Jia, M. Gu, and C. Du, "Three-dimensional nanoscale far-field focusing of radially polarized light by scattering the SPPs with an annular groove," Opt. Express **18**(14), 14664–14670 (2010).
23. C. J. Powell, "Analysis of optical- and inelastic-electron-scattering data. II. application to Al," J. Opt. Soc. Am. **60**(1), 78–93 (1970).
24. S. Bourzeix, J. M. Moison, F. Mignard, F. Barthe, A. C. Boccara, C. Licoppe, B. Mersali, M. Allovon, and A. Bruno, "Near-field optical imaging of light propagation in semiconductor waveguide structures," Appl. Phys. Lett. **73**(8), 1035–1037 (1998).
25. X. Li, T.-H. Lan, C.-H. Tien, and M. Gu, "Three-dimensional orientation-unlimited polarization encryption by a single optically configured vectorial beam," Nat. Commun. **3**, 998 (2012).

1. Introduction

Finite length silver (Ag) nanowires (NWs) are intriguing plasmonic structures due to their strong polarizibility compared with the spherical shaped structures and a low loss among the metallic NWs [1]. These kinds of anisotropic extended Ag nanostructures with sub-wavelength dimensions can support propagating surface plasmons (SPs) along the NW with a lateral confinement in the other two directions and with a micro-scale propagation length thereby acting as sub-wavelength plasmonic waveguides [2]. In addition, controlling the order and the polarization properties of the plasmonic modes in free-standing Ag NWs has enabled a wide range of applications such as beam splitters, polarization rotators, bio-sensors and so on [3–6]. On the other hand, Ag NWs on a dielectric substrate have been widely studied [7, 8], owing to the relatively longer propagation length, stronger energy confinement and the enhanced evanescent field at the interface compared to the free-standing NW, which opens up the possibility for novel and high performance miniaturized optical devices [9, 10]. The presence of the substrate can break up the symmetry and fundamentally change the plasmonic modes supported in the hybrid structure. Thus the NW waveguide on the substrate can turn into a single-mode operation [10, 11], which is crucial for practical optical waveguide applications. Because of its sensitivity to the evanescent wave and high spatial resolution, the scanning optical near-field microscope (SNOM) is widely used to study the localized plasmonic modes in Ag NWs [12, 13]. However, the near-field studies of Ag NWs are mainly focused on the intensity distribution [14, 15]. The polarization properties of the plasmonic modes in Ag NWs on a dielectric substrate are yet to be determined, but are necessary prior to its practical applications.

In this paper, we report on the near-field analysis of the polarization properties of the propagating plasmonic modes along the NW on a glass substrate. The far-field result reveals the existence of two orthogonal polarization components of the plasmonic mode at the distal end. The near-field mapping of the propagating plasmonic modes of the NW on the substrate by a SNOM probe with an in-plane polarization-sensitivity provides a further insight into the two polarization components.

2. Experimental setup and far-field characterization

The experimental setup for the far-field and near-field characterization of the plasmonic mode is shown in Fig. 1(a). Propagating plasmonic modes can be excited at one end of an Ag NW by the focal optical field irradiation [16, 17], due to the symmetry breaking at the excitation end of the NW [18]. The Ag NWs are commercially available with a diameter of ~150 nm (± 10 nm) and a length of ~7 μm (± 0.2 μm). Figure 1(b) shows a scanning electron microscope image of the typical example of the NW. The incident laser beam at a wavelength

#190145 - $15.00 USD Received 6 May 2013; revised 9 Jun 2013; accepted 11 Jun 2013; published 18 Jun 2013

of 632.8 nm (He-Ne laser) is focused by a high numerical aperture (NA = 1.4) oil immersion objective, to one end facet of the Ag NW on a cover glass (R.I = 1.46) [19]. The polarization angle (θ, defined as the polarization orientation with respect to the axis of the NW) of the incident beam is changed by rotating a half wave plate placed after the linear polarizer. The incident laser beam is coupled to the NW as propagating SPs. The SPs at the distal end is scattered to the far-field and imaged by the same objective with a CCD camera. When the input polarization is parallel to the orientation of the NW, the depolarized longitudinal field components induced by the tight focusing with a high NA objective, match well with the electric field distribution of the single mode in the NW which is highly polarized along the longitudinal direction. This feature leads to the maximal coupling efficiency producing a bright spot at the distal end of the NW (Fig. 1(c)). When the input polarization is perpendicular to the orientation of the NW, the longitudinal field components do not match with the electric field distribution of the mode leading to a minimal coupling efficiency and thereby producing a dark spot at the distal end of the wire (Fig. 1(d)). This observation is consistent with a previous report [12]. The dependence of the scattering intensity at the distal end of the NW on the incident polarization orientation can be seen clearly in Fig. 1(e).

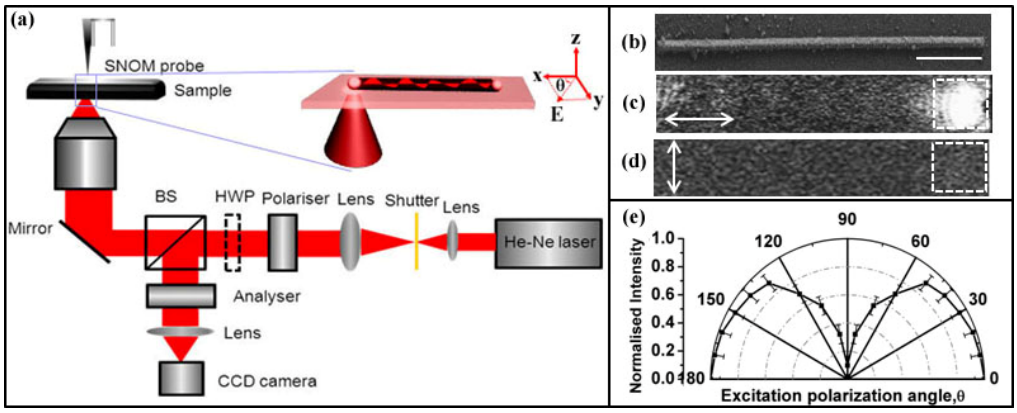

Fig. 1. (a) The experimental setup for the far-field and near-field characterization of the polarization components of the plasmonic mode and the schematic illustration of excitation of the Ag NW on a substrate. The incident beam with an electric field, E with an incident wave vector, K and a polarisation angle (θ) is focused on one facet of the Ag NW. (b) Scanning electron microscopy image of the NW. (c) and (d) show the bright and dark spots at the distal end for the parallel and perpendicular incident polarization orientations, respectively (The scale bar is 2μm and the double headed arrows indicate the incident polarization orientation). (e) Emission intensity from the distal end of the NW as a function of the excitation polarization angle (θ).

To analyze the polarization state at the distal end, a polarization analyzer was placed in front of the CCD. The dependence of the emission intensity at the distal end under three different incident polarization orientations on the direction of the analyzer is shown in Fig. 2(a). In the current experimental geometry, only a single mode can be supported in the NW. Thus, the ratio of the scattered intensities in the two orthogonal directions is a characteristic of the single mode, which is independent of the input polarization. At the distal end, the intensity in the parallel direction is 2.5 times stronger than that in the perpendicular direction, which might be attributed to the additional contribution from the depolarized transverse fields collected by the high NA objective. The output polarization is sensitive to the shape of the distal end when high-order modes exist in the NW [16]. In contrast to the multimode case, the observed far-field polarization in the distal end is dominantly parallel to the direction of the NW, which is a characteristic of the single mode. As the analyzer in front of the CCD detector is rotated, different polarization components is observed. The parallel (when the direction of the analyzer is parallel to the axis of the NW) and perpendicular (when the analyzer is perpendicular to the axis of the NW) polarization observed in Figs. 2(b) and 2(c)

#190145 - $15.00 USD Received 6 May 2013; revised 9 Jun 2013; accepted 11 Jun 2013; published 18 Jun 2013

are the scattered electric fields of the NW and collected by the objective. Figures 2(b) and 2(c) therefore correspond to the parallel electric fields located in the center of the NW and the perpendicular electric fields distributed along the edge of the NW, respectively. The different intensity distributions in Figs. 2(b) and 2(c) indicate that these field components originate from two different polarization components with different spatial distributions.

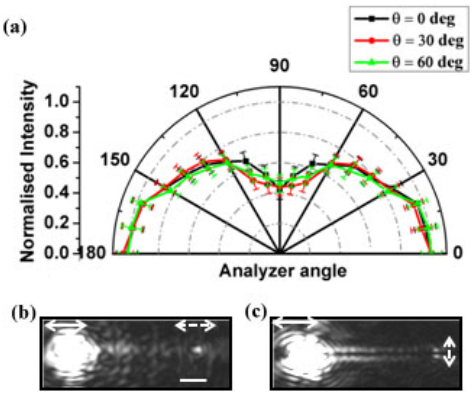

Fig. 2. (a) Emission intensity from the distal end of the NW as a function of the analyzer angle for different excitation polarization orientations with respect to the axis of the NW. Plasmonic mode distribution on the Ag NW when the analyzer in front of the CCD detector is (b) parallel and (c) perpendicular to the axis of the NW (The scale bar is 2μm, the double headed arrows indicate the excitation polarization orientation and the dashed arrows indicate the direction of analyzer).

3. Near-field characterization

To verify the two polarization components of the plasmonic modes, we conducted a near-field mapping of the propagating mode along the Ag NW. A SNOM probe exhibiting a preferred polarization sensitive direction was employed in the characterization, which has been discovered in a previous report that the polarization-sensitivity of the tip is related to the shape of the aperture. In the measurement, we used a commercially available SNOM probe (Nufern fibre probe, NT-MDT) with an Aluminium coating of a thickness of 50 nm. The measured aspect ratio of the aperture of the probe is ~2:1, indicating an elliptical shape. The elliptical shape induced preferential transmission for light with different polarization states has also been observed in the previous report [20]. To quantify the directional polarization-sensitivity, the probe was scanned across the focal spot of a linearly polarized beam focused by an objective lens (NA = 0.7). The input polarization was rotated from 0° to 180° by using a half wave plate. As shown in Fig. 3(a), the probe showed a ~10 times higher sensitivity along one direction than the perpendicular direction. To further confirm this in-plane polarization-sensitivity, we used the probe to scan the focal spot of a plasmonic lens [21, 22] with linearly polarized excitation along the x-axis. The field distribution of the focal spot was measured when the polarization-sensitive direction of the probe was parallel (Fig. 3(b)) and perpendicular (Fig. 3(c)) to the excitation polarization, respectively. The near-field optical images obtained were consistent with the simulated field components obtained from finite element method (COMSOL Multiphysics), and revealed clearly the $|E_x|^2$ and $|E_y|^2$ in-plane components of the focal spot (Figs. 3(d)-3(f)). As such, this probe can be used to study the two orthogonal polarization components of the Ag NWs.

#190145 - $15.00 USD Received 6 May 2013; revised 9 Jun 2013; accepted 11 Jun 2013; published 18 Jun 2013

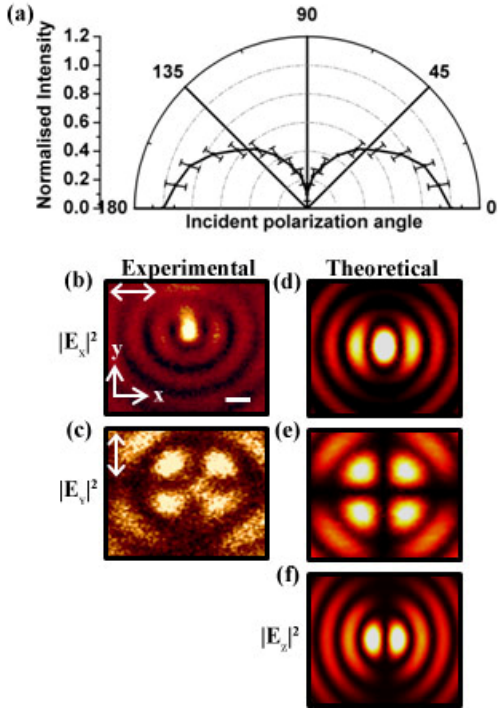

Fig. 3. (a) The intensity of the focal spot of an objective lens by an in-plane polarization sensitive probe as a function of the incident polarization rotation angle. Comparison of the simulated focal spots of a plasmonic lens obtained by COMSOL and experimentally obtained by a polarization sensitive SNOM probe. The SNOM optical images when the preferred polarization sensitive direction of the probe is (b) parallel and (c) perpendicular to the excitation direction. Simulation result of the transverse components (d, e) and the longitudinal component (f) of the plasmonic lens at the focal plane (The scale bar is 350 nm and the two headed arrows indicate the direction of probe sensitivity).

For the near-field characterization of the polarization components of the plasmonic mode by the in-plane polarization sensitive probe, the incident polarization was aligned parallel to the axis of the NW along x-coordinate. The transverse mode imaging was obtained when the probe sensitive direction was rotated parallel and perpendicular to the axis of the NW (Figs. 4(a) and 4(b)), respectively. Indeed, the images show two orthogonal polarization components. The x-polarized component is located at the center of the NW, while the y-polarized component is at the edge of the NW. The high resolution of the SNOM allows the existence of the periodic peaks due to the interference of the propagating plasmonic modes along the NW. The same periodicity between two polarization components is revealed, indicating that they are two polarization components of the same order of modes, which is consistent with the previous report [10].

For a comparison, we employed the finite element method to simulate the field distribution under the same excitation condition. The excitation geometry was depicted in Fig. 1(a) with a Gaussian excitation beam. Optical constants of Ag at wavelength 632.8 nm are taken as refractive index, R.I = 0.1437 + *i*3.8082 [23]. In our case, only the first order modes was excited due to the symmetry breaking when the NW was on the glass substrate [10]. The electric field components of the plasmonic modes in x and y-directions are shown in Figs. 4(c) and 4(d), respectively. The separation of the intensity peaks is measured as 350 nm, which is slightly larger than the simulation result of 250 nm. This discrepancy might be attributed to the Tien effect [24] considering the refractive-index gradient in the radial direction caused by the quick oxidation of the surface of the Ag NW in air. While, the qualitative agreement between the simulation and experimental results confirms that

#190145 - $15.00 USD Received 6 May 2013; revised 9 Jun 2013; accepted 11 Jun 2013; published 18 Jun 2013

individual polarization components have been revealed distinctively by the in-plane sensitive probe.

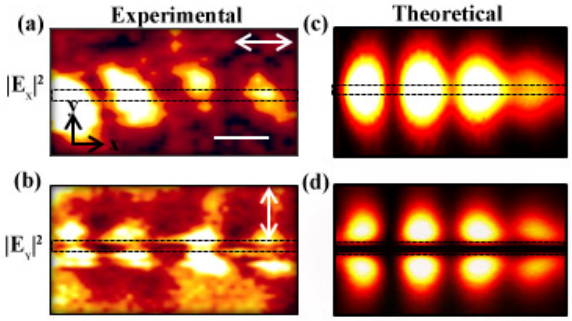

Fig. 4. Near-field optical imaging of the propagating plasmonic mode along the Ag NW when the preferred polarization sensitive direction of the SNOM probe is rotated in (a) parallel and (b) perpendicular to the axis of the NW (black dotted line indicates the NW orientation). Simulation result of (c) $|E_x|^2$ and (d) $|E_y|^2$ components of the distribution of the plasmonic mode (The scale bar is 350 nm and the two headed arrows indicate the direction of probe sensitivity).

4. Conclusion

In conclusion, we have experimentally investigated the polarization components of the propagating plasmonic mode of the Ag NW waveguide on a glass substrate by the scanning near-field optical microscope. Experimental results in the near-field mapping by an in-plane polarization sensitive probe reveal two orthogonal polarization components of the plasmon modes along the axis of the NW. Our results constitute a comprehensive polarization study of the propagating plasmonic mode of an Ag NW on a dielectric substrate. The polarization feature of the hybrid NW structure discovered here may open up a new avenue for developing polarization-sensitive applications [25] such as optical nano-polarizers.

Acknowledgment

This work was supported by the Australian Research Council (ARC) Laureate Fellowship scheme (FL100100099).

#190145 - $15.00 USD Received 6 May 2013; revised 9 Jun 2013; accepted 11 Jun 2013; published 18 Jun 2013